

Electronic Supplementary Information (ESI)

Hexagonal array formation by intermolecular halogen bonding using a binary blend of linear building blocks: STM study

Yoshihiro Kikkawa,* Mayumi Nagasaki, Emiko Koyama, Seiji Tsuzuki and Kazuhisa Hiratani

National Institute of Advanced Industrial Science and Technology (AIST), Tsukuba Central 5, 1-1-1 Higashi, Tsukuba, Ibaraki 305-8565, Japan

SI 1. Experimental details

SI 2. Lattice constants of 2D structures

SI 3. STM images of the binary blend ($p1+2$) at the higher concentration

SI 4. Analysis of STM images in Fig. 2 ($p1+2$)

SI 5. Proposed molecular arrangements of the binary blend ($p1+2$)

SI 6. Proposed molecular arrangements of the binary blend ($m1+2$)

SI 7. Orientation of $m1$ and 2 in the binary blend ($m1+2$)

SI 8. STM images of 3

SI 9. 2D chirality in the binary blend ($m1+2$)

SI 10. Additional STM images of the binary blend ($m1+2$)

SI 11. Concentration-dependent 2D structures

SI 12. Statistical analysis of the 2D structure formation

SI 1. Experimental details

The chemicals used in this study were purchased from Sigma-Aldrich, Kanto, or Tokyo Chemical Industry and used without further purification. The prepared compounds were characterized using NMR (Bruker Avance 500 spectrometer) and FT-IR (JASCO FT/IR420) using KBr pellets. High-resolution matrix-assisted laser desorption/ionization time-of-flight mass (HR-MALDI-TOF-MS) was performed by using a JMS-S3000 MALDI spiral TOF-MS. Trans-2-[3-(4-tert-Butylphenyl)-2-methyl-2-propenylidene]malononitrile (DCTB) was used for the matrix.

Preparation of the building blocks p1 and m1

4-((3,4-bis(octadecyloxy)phenyl)ethynyl)pyridine (p1)

1,2-bis(octadecyloxy)-4-iodobenzene was prepared using a similar procedure reported previously.^{S1} To a solution of 4-ethynylpyridine (Tokyo Chemical Industry: 0.031 g, 0.3 mmol) in THF (60 ml) was added 1,2-bis(octadecyloxy)-4-iodobenzene (0.266 g, 0.36 mmol), Pd(PPh₃)₄ (0.021 g, 0.018 mmol), CuI (0.008 g, 0.018 mmol) and triethylamine (30 ml). The flask was cooled, degassed, charged with N₂ gas, and stirred at 60 °C for 9 days. Then, the solvent was evaporated in vacuo, and the residue was extracted with CHCl₃ and dried over anhydrous MgSO₄. The crude product was purified by silica gel column chromatography with CHCl₃ as an eluent, and recrystallized from CHCl₃/MeOH. A light yellow solid was obtained in 37 % yield.

¹H NMR (CDCl₃): δ 0.88 (t, *J* = 6.93 Hz, 6H), 1.26 (br, 32H), 1.46 (m, 4H), 1.83 (m, 4H), 4.01 (m, 4H), 6.84 (d, *J* = 8.35 Hz, 1H), 7.04 (d, *J* = 1.85 Hz, 1H), 7.12 (dd, *J*₁ = 8.30 Hz, *J*₂ = 2.00 Hz, 1H), 7.35 (d, *J* = 6.10 Hz, 2H), 8.58 (d, *J* = 6.00 Hz, 2H). ¹³C NMR (CDCl₃): δ 14.1, 22.7, 26.0, 29.2, 29.4, 29.7, 31.9, 69.2, 69.4, 85.3, 94.7, 113.2, 114.0, 116.8, 125.5, 131.9, 148.8, 149.7, 150.6. IR (KBr): 2918, 2849, 1590, 1519, 1468, 1260, 1228, 1128 cm⁻¹. MS (HR-MALDI-TOF MS): *m/z* calculated for C₄₉H₈₁NO₂⁺, 715.6262; found, 715.6280.

3-((3,4-bis(octadecyloxy)phenyl)ethynyl)pyridine (m1)

The 3-ethynylpyridine (Tokyo Chemical Industry) was used for the preparation of **m1**. The procedure was the same as **p1**, and purified with GPC. The target compound was obtained as a white solid in 85% yield.

¹H NMR (CDCl₃): δ 0.88 (t, *J* = 6.90 Hz, 6H), 1.26 (br, 32H), 1.46 (m, 4H), 1.82 (m, 4H), 4.01 (t, *J* = 6.65 Hz, 4H), 6.84 (d, *J* = 8.35 Hz, 1H), 7.04 (d, *J* = 1.90 Hz, 1H), 7.11 (dd, *J*₁ = 8.25 Hz, *J*₂ = 1.90 Hz, 1H), 7.28 (m, overlapped with CHCl₃, 1H), 7.78 (d, *J* = 7.90 Hz, 1H), 8.53 (d, *J* = 4.00 Hz, 1H), 8.75 (s, 1H). ¹³C NMR (CDCl₃): δ 14.1, 22.7, 26.0, 29.2, 29.7, 31.9, 69.2, 84.4, 93.1, 113.2, 114.5, 116.6, 120.8, 123.0, 125.2, 138.2, 148.2, 148.8, 150.2, 152.2. IR (KBr): 2917, 2849, 1514, 1464, 1254, 1220, 1126 cm⁻¹. MS (HR-MALDI-TOF MS): *m/z* calculated for C₄₉H₈₁NO₂⁺, 715.6262; found, 715.6280.

Preparation of the building block 2

Methyl 3,5-bis(octadecyloxy)benzoate

To a solution of methyl 3,5-dihydroxybenzoate (3.36 g, 20 mmol) and K₂CO₃ (6 g, 43 mmol) in DMF was added 1-bromooctadecane (15 g, 45 mmol), and stirred at 170 °C for 24 hr. After the evaporation of the solvent under reduced pressure, the product was purified by silica gel column chromatography with CHCl₃/n-hexane (volume ratio 1/3) as an eluent. The compound was obtained as a white solid in 87% yield.

¹H NMR (CDCl₃): δ 0.88 (t, *J* = 6.95 Hz, 6H), 1.26 (br, 60H), 1.44 (m, 4H), 1.77 (m, 4H), 3.89 (s, 3H), 3.96 (t, *J* = 6.56 Hz, 4H), 6.63 (dd, *J* = 2.33, 2.33 Hz, 1H), 7.04 (d, *J* = 2.40 Hz, 2H).

3,5-bis(octadecyloxy)benzylalcohol

To a stirred suspension of LiAlH₄ (1.3 g, 34 mmol) in diethylether was added a solution of the methyl 3,5-bis(octadecyloxy)benzoate (11.5 g, 17 mmol) in THF at 0 °C with N₂ bubbling. Then,

the mixture was stirred at room temperature for 1 hr. The reaction was quenched by slow addition of water and 15% aqueous NaOH. The insoluble part was filtered, and the solution was evaporated under the reduced pressure. The product was purified by silica gel column chromatography with CHCl₃ as an eluent, and the compound was received as white solid in 62 % yield.

¹H NMR (CDCl₃): δ 0.88 (t, J = 6.90 Hz, 6H), 1.26 (br, 60H), 1.44 (m, 4H), 1.57 (t, J = 5.90 Hz, 1H), 1.76 (m, 4H), 3.93 (t, J = 6.55 Hz, 4H), 4.62 (d, J = 6.10 Hz, 2H), 6.38 (dd, J = 2.15, 2.15 Hz, 1H), 6.49 (d, J = 1.85 Hz, 2H).

1-((3,5-bis(octadecyloxy)benzyl)oxy)-2,3,5,6-tetrafluoro-4-iodobenzene (2)

To a solution of 3,5-bis(octadecyloxy)benzylalcohol (1.2 g, 1.86 mmol) in small amount of DMF (0.5 ml) was added Cs₂CO₃ (0.61 g, 1.86 mmol), and the solution was stirred at 80 °C for 1 hr. Then, the perfluoroiodobenzene was added to the reaction mixture, and stirred at 80 °C for 1 hr. After the evaporation of the solvent in vacuo, the reaction mixture was extracted with CHCl₃, and the solution was dried over anhydrous MgSO₄. Then, the crude product was purified by silica gel column chromatography with CHCl₃ as an eluent.

¹H NMR (CDCl₃): δ 0.88 (t, J = 6.95 Hz, 6H), 1.26 (br, 60H), 1.43 (m, 4H), 1.76 (m, 4H), 3.92 (t, J = 6.58 Hz, 4H), 5.18 (s, 2H), 6.41 (dd, J = 2.20, 2.20 Hz, 1H), 6.49 (d, J = 2.15 Hz, 2H). ¹³C NMR (CDCl₃): δ 14.1, 22.7, 26.0, 29.2, 29.4, 29.6, 29.7, 31.9, 68.2, 101.9, 106.4, 137.3, 160.5. ¹⁹F NMR (CDCl₃): δ -121.4 to -121.3 (m, 2F), -153.3 to -153.2 (m, 2F). IR (KBr): 2919, 2850, 1599, 1489, 1378, 1159, 1096 cm⁻¹. MS (HR-MALDI-TOF MS): *m/z* calculated for C₄₉H₇₉F₄IO₃Na, 941.4902 [M+Na]⁺; found, 941.4891.

Preparation of the 3

The compound **3** (1-((3,4-bis(octadecyloxy)benzyl)oxy)-2,3,5,6-tetrafluoro-4-iodobenzene) was prepared with the same method as **2**, excepting the substitution position of the starting material.

^1H NMR (CDCl_3): δ 0.88 (t, $J = 6.95$ Hz, 6H), 1.26 (br, 60H), 1.45 (m, 4H), 1.80 (m, 4H), 3.98 (m, 4H), 5.18 (s, 2H), 6.49 (d, $J = 8.15$ Hz, 1H), 6.81 (d, $J = 8.2$ Hz, 1H), 6.95 (s, 1H). ^{13}C NMR (CDCl_3): δ 14.1, 22.7, 26.1, 29.3, 29.4, 29.5, 29.7, 32.0, 68.3, 68.4, 103.4, 114.3, 121.6, 127.8, 149.3, 150.0. ^{19}F NMR (CDCl_3): δ -121.6 to -121.5 (m, 2F), -153.3 (m, 2F). IR (KBr): 2919, 2850, 1592, 1486, 1377, 1140, 1088 cm^{-1} . MS (HR-MALDI-TOF MS): m/z calculated for $\text{C}_{49}\text{H}_{79}\text{F}_4\text{IO}_3\text{Na}$, 941.4902 $[\text{M}+\text{Na}]^+$; found, 941.4904.

STM at solid/liquid interface

The components **1** and **2** were dissolved in 1-phenyloctane at different concentrations, and the solution was deposited on a HOPG surface to form a physisorbed monolayer. In the case of bicomponent blend, the 1-phenyloctane solution of the components were pre-mixed at 1:1 ratio, and the mixed solution was placed on the HOPG surface. A Pt/Ir wire (90/10: 0.25 mm ϕ) was cut to prepare the STM tip, which was immersed in the droplet on the HOPG surface. The STM images were recorded in the low current mode STM (Nanoscope IIIa, Digital Instruments) at the HOPG/1-phenyloctane interface. The obtained STM images were corrected by using the HOPG lattice underneath the monolayer, and processed by the SPIP software.

DFT calculations

Gaussian 09 program^{S2} was used for geometry optimizations and calculations of the stabilization energies associated with the formation of interdigitated structures from isolated species. The 6-311G** basis set and B97D functional were used for the calculations.^{S3}

SI 2. Lattice constants of 2D structures

Table S1 Lattice constants measured from the STM images in Figs. 1-3 and S6.

	a (nm)	b (nm)	γ (deg)	Ref.
$p1$	1.35 ± 0.02	4.43 ± 0.08	88 ± 2	Fig. 1A
$m1$	1.40 ± 0.13	4.45 ± 0.08	86 ± 2	Fig. 1B
2	1.36 ± 0.11	5.12 ± 0.19	85 ± 4	Fig. 1C
3	1.76 ± 0.06	3.54 ± 0.02	89 ± 1	Fig. S6
$p1 + 2$	1.80 ± 0.06	4.33 ± 0.15	85 ± 1	Fig. 2A
$m1 + 2$	7.47 ± 0.14	7.47 ± 0.14	61 ± 1	Fig. 3A

SI 3. STM images of the binary blend ($p1+2$) at the higher concentration

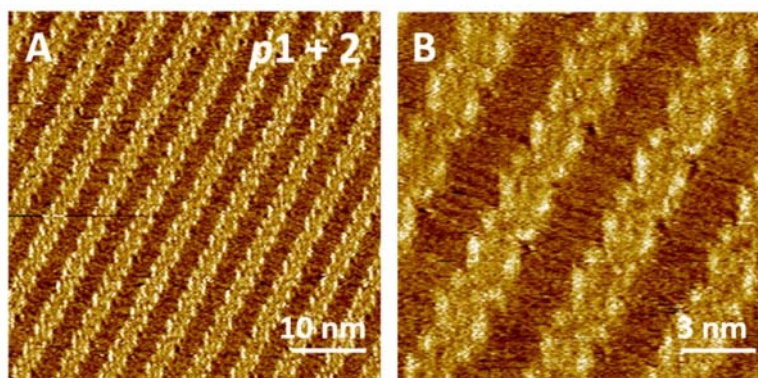


Fig. S1 STM images of the bicomponent blend of $p1$ and 2 (0.25 mM) observed at the HOPG/1-phenyloctane interface. The present double columnar structure was observed in addition to the linear structure in Fig. 2. Tunnelling conditions: (A) $I = 1.0$ pA, $V = -713$ mV, (B) $I = 1.0$ pA, $V = -713$ mV.

SI 4. Analysis of STM images in Fig. 2 ($p1+2$)

The column widths were measured to further analyse the 2D structures in Figs. 1A, 1B and 2A. In Fig. S2A, the width of the double columnar structure for $p1$ (w_{p1}) was measured to be 2.15 ± 0.14 nm, whereas that of w_2 perpendicular to the column long axis (Fig. S2B) was 1.87 ± 0.17 nm. Although the measured lengths of L_1 , L_3 (L_4), and L_5 was almost identical (ca. 2.2 nm) because they are corresponding to the length of C18 alkyl chain, the column width of the bicomponent blend of $p1$ and 2 (w_{p1+2}) in Fig. S2C was measured as 1.99 ± 0.13 nm, which was slightly different from both w_{p1} and w_2 . In addition, the distance between the short stick-like structures (d_{p1+2}) was measured to be 0.90 ± 0.03 nm (Fig S2D), which was smaller than the lattice constant of $p1$ (1.35 ± 0.02 nm) and 2 (1.36 ± 0.11 nm) along the a -axis. These analyses suggest that the bicomponent blend of $p1$ and 2 ($p1 + 2$) formed the linear 2D structure, which is different from both $p1$ and 2 . The 2D structure of $p1 + 2$ can be formed via intermolecular interactions shown in Fig. S3.

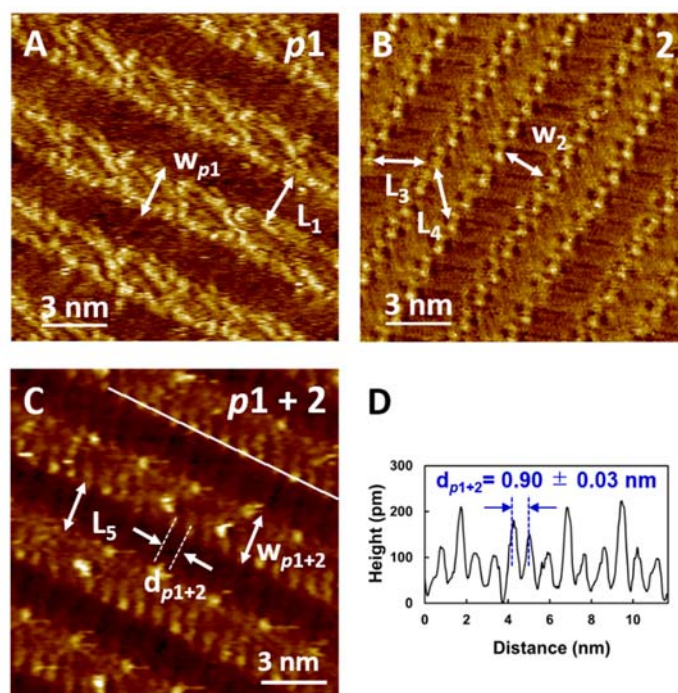


Fig. S2 STM images of $p1$ (A), 2 (B) and the bicomponent blend of $p1 + 2$ (C). The panel (D) shows the cross-sectional data at the white lined region in (C).

SI 5. Proposed molecular arrangements of the binary blend (*p1*+*2*)

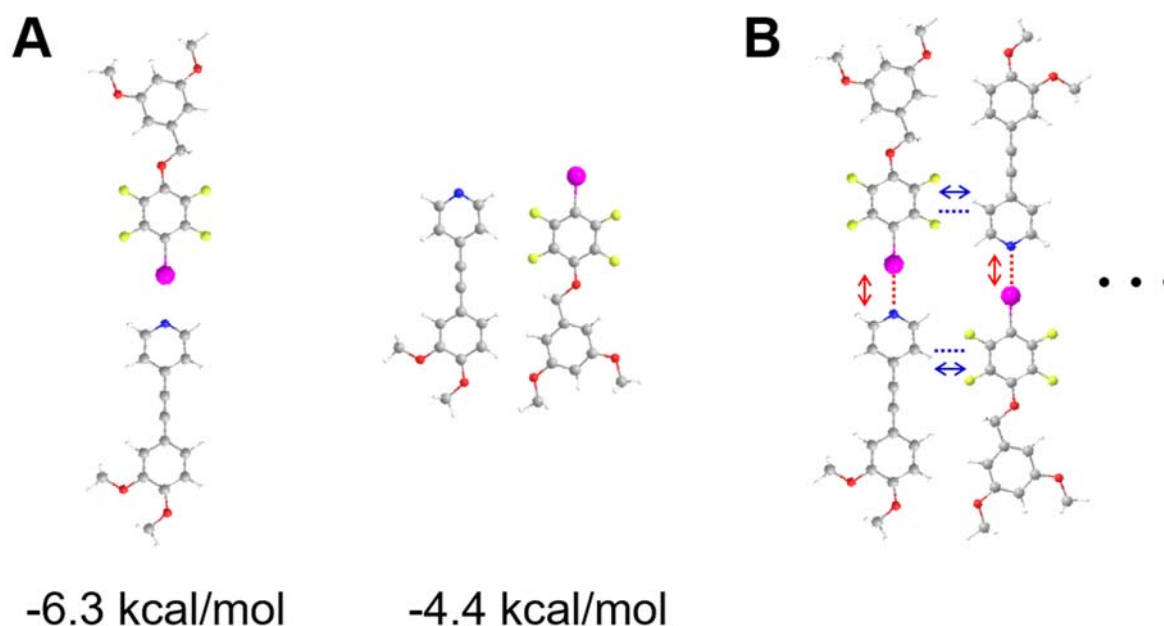


Fig. S3 (A) Optimized structures of the complex of model molecules *p1Me* and *2Me* in which the C18 alkyl chains of *p1* and *2* have been replaced with methyl groups, along with the stabilization energies associated with the formation of the complexes obtained by DFT calculations. The stabilization energies calculated for the structures were comparable to that of a typical hydrogen bond (4–6 kcal/mol)^{S4}. (B) Plausible structure for the complex composed of two *p1Me* and two *2Me* molecules based on the intermolecular interactions that were observed in the two optimized structures of the complexes of *p1Me* and *2Me*. The red arrow is an I...N halogen bond, whereas the blue one indicates an intermolecular interaction between the negatively charged peripheral fluorine atoms in the 2,3,5,6-fluoroiodobenzene moiety of *2Me* and the positively charged hydrogen atoms in the pyridine ring of *p1Me* (Ar-F...H-Py interaction).

SI 6. Proposed molecular arrangements of the binary blend ($m1+2$)

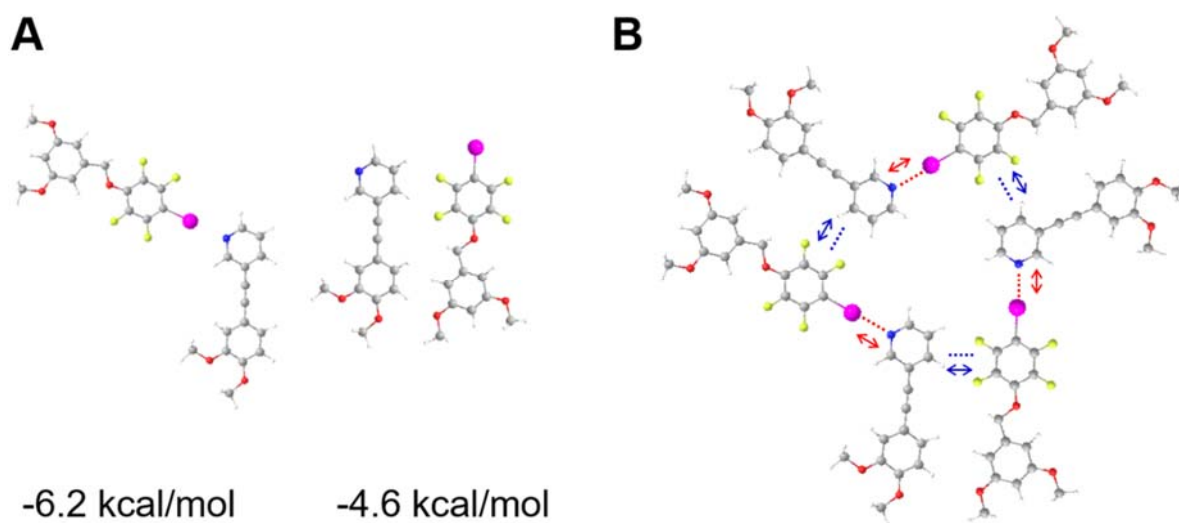


Fig. S4 (A) Optimized structures of the complex of the model molecules ***m1Me*** and ***2Me*** in which the C18 alkyl chains of ***m1*** and ***2*** have been replaced with methyl groups, along with the stabilization energies associated with the formation of the complexes, as obtained by DFT calculations. (B) A plausible structure for the triangular helical assemblies composed of three ***m1Me*** and three ***2Me*** based on the intermolecular interactions indicated by the red (I...N halogen bond) and blue arrows (Ar-F...H-Py interaction between ***2Me*** and ***m1Me***).

SI 7. Orientation of *m1* and *2* in the binary blend (*m1+2*)

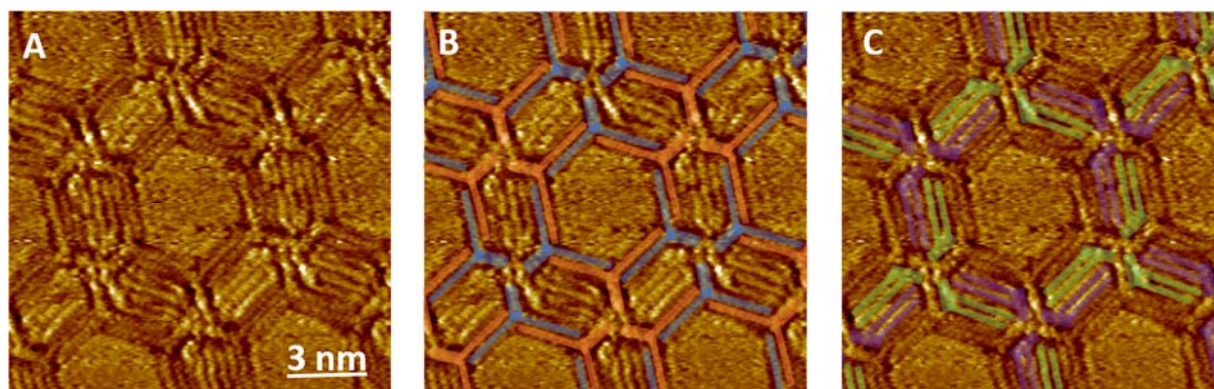


Fig. S5 STM images of the hexagonal arrays. The building block **2** is indicated by blue and red (B), whereas ***m1*** is shown in green and purple (C) to highlight the conformations of the molecules as well as their arrangement. The alkyl chains of **2** are clearly in an expanded conformation (B) similar to those of the mono-component system (Fig. 1C), and the alkyl chains in ***m1*** are aligned parallel to one another (C). Tunnelling conditions: $I = 2.0$ pA, $V = -353$ mV.

SI 8. STM images of **3**

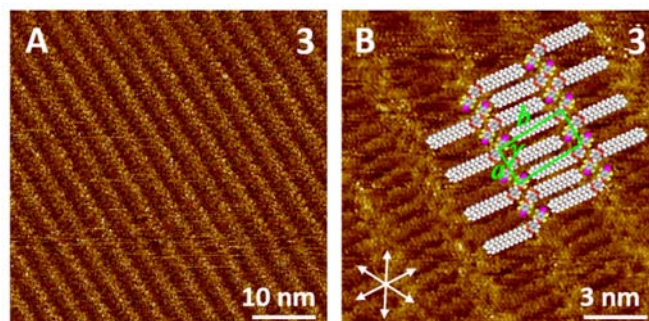


Fig. S6 STM images of **3** at the HOPG/1-phenyloctane interface. The set of arrows indicate the HOPG lattice direction. Tunnelling conditions: (A) $I = 10$ pA, $V = -684$ mV, (B) $I = 10$ pA, $V = -736$ mV.

SI 9. 2D chirality in the binary blend ($m1+2$)

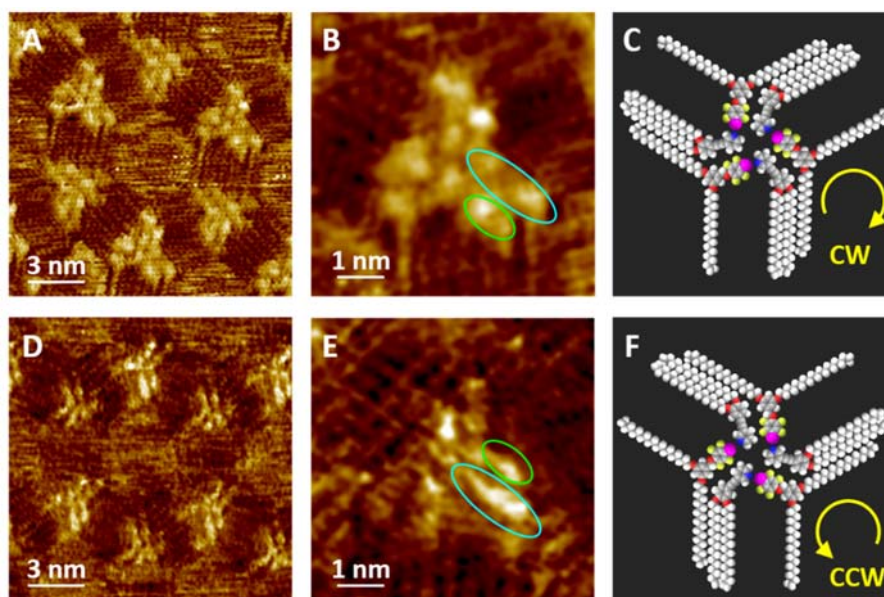


Fig. S7 STM images of the hexagonal arrays, in which the triangular assemblies show CW (A) and CCW helicities (D). Panels (B) and (E) are enlargements of regions of (A) and (D), respectively. The bar-like structures marked with green and blue circles are oriented in a chiral fashion. Panels (C) and (F) are the proposed molecular models based on the STM images. Tunnelling conditions: (A) $I = 1.0$ pA, $V = -650$ mV, (D) $I = 1.0$ pA, $V = -103$ mV.

SI 10. Additional STM images of the binary blend ($m1+2$)

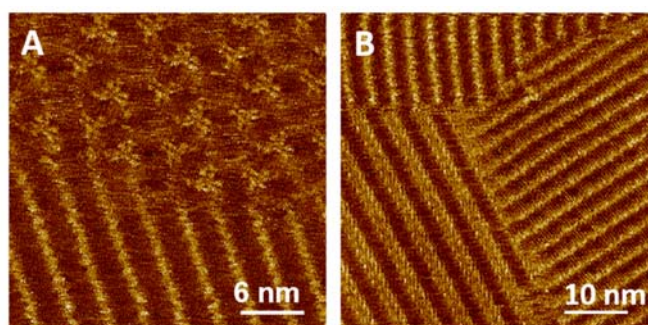


Fig. S8 STM images of the borders between two different domain structures in the bicomponent blend of $m1$ and 2 . In panel (A), domains composed of hexagonal arrays and linear structures are present, whereas double columnar and single-lined structures are found in panel (B). Tunnelling conditions: (A) $I = 1.0$ pA, $V = -242$ mV, (B) $I = 1.0$ pA, $V = -36$ mV.

SI 11. Concentration-dependent 2D structures

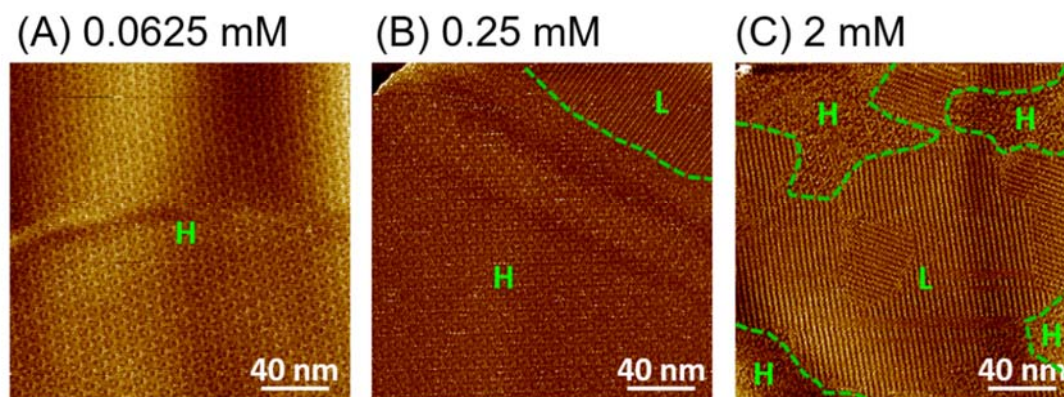


Fig. S9 STM images of the bicomponent blend of *m1* and *2* at different concentrations. H: hexagonal array, L: linear structure. Tunnelling conditions: (A) $I = 1.0$ pA, $V = -42$ mV, (B) $I = 1.0$ pA, $V = -136$ mV, (C) $I = 1.0$ pA, $V = -30$ mV.

SI 12. Statistical analysis of 2D structure formation

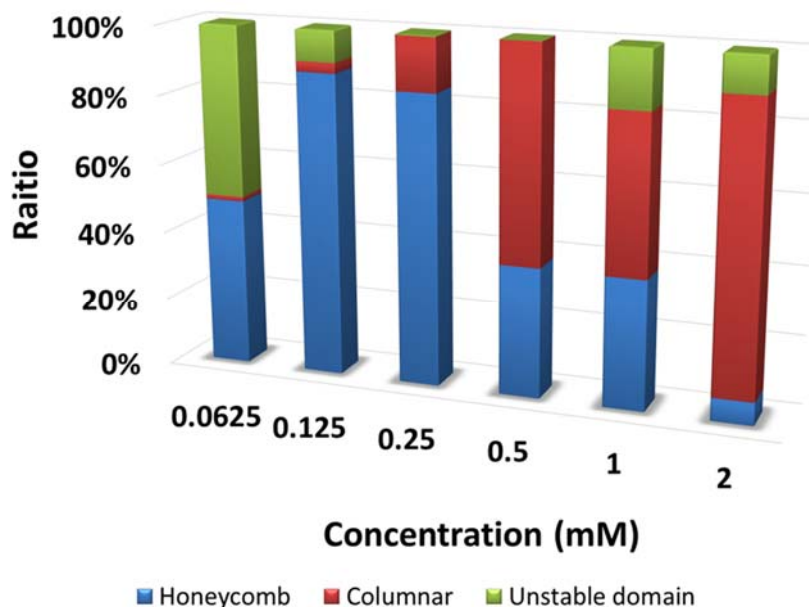


Fig. S10 Bar graph showing the ratios of the different 2D structures at different concentrations. The ratio was measured from ten different STM images with dimensions of $200 \text{ nm} \times 200 \text{ nm}$. The “columnar structure” (red) includes both the double columnar and linear structures. The “unstable domain” (green) indicates fuzzy regions whose 2D structure was difficult to identify.

References

- S1. Y. Kikkawa, E. Koyama, S. Tsuzuki, K. Fujiwara, K. Miyake, H. Tokuhisa and M. Kanosato, *Langmuir*, 2006, **22**, 6910.
- S2. Gaussian 09, Revision C01, M. J. Frisch, G. W. Trucks, H. B. Schlegel, G. E. Scuseria, M. A. Robb, J. R. Cheeseman, G. Scalmani, V. Barone, B. Mennucci, G. A. Petersson, H. Nakatsuji, M. Caricato, X. Li, H. P. Hratchian, A. F. Izmaylov, J. Bloino, G. Zheng, J. L. Sonnenberg, M. Hada, M. Ehara, K. Toyota, R. Fukuda, J. Hasegawa, M. Ishida, T. Nakajima, Y. Honda, O. Kitao, H. Nakai, T. Vreven, J. A. Montgomery, Jr., J. E. Peralta, F. Ogliaro, M. Bearpark, J. J. Heyd, E. Brothers, K. N. Kudin, V. N. Staroverov, R. Kobayashi, J. Normand, K. Raghavachari, A. Rendell, J. C. Burant, S. S. Iyengar, J. Tomasi, M. Cossi, N. Rega, J. M. Millam, M. Klene, J. E. Knox, J. B. Cross, V. Bakken, C. Adamo, J. Jaramillo, R. Gomperts, R. E. Stratmann, O. Yazyev, A. J. Austin, R. Cammi, C. Pomelli, J. W. Ochterski, R. L. Martin, K. Morokuma, V. G. Zakrzewski, G. A. Voth, P. Salvador, J. J. Dannenberg, S. Dapprich, A. D. Daniels, Ö. Farkas, J. B. Foresman, J. V. Ortiz, J. Cioslowski, and D. J. Fox, Gaussian, Inc., Wallingford CT, 2009
- S3. S. Grimme, *J. Comp. Chem.*, 2006, 27, 1787.
- S4. M. –H. Hao, *J. Chem. Theory Comput.* 2006, **2**, 863.